

A light-triggerable nanoparticle library for the controlled release of non-coding RNAs

Josephine Blersch¹, Vitor Francisco^{1,2}, Catarina Rebelo^{1,2}, Adrian Jiménez-Balsa¹, Helena Antunes^{1,2}, Carlo Gonzato³, Sandra Pinto¹, Susana Simões¹, Klaus Liedl⁴, Karsten Haupt³, Lino Ferreira^{1,2*}

¹Center for Neuroscience and Cell Biology, University of Coimbra, Coimbra, Portugal

²Faculty of Medicine, University of Coimbra, 3000-548, Coimbra, Portugal

³Sorbonne Universités, Université de Technologie de Compiègne, Laboratory for Enzyme and Cell Engineering UMR CNRS 7025, 60200 Compiègne, France

⁴Faculty of Chemistry and Pharmacy, Leopold-Franzens, University Innsbruck, Austria

ABSTRACT

RNA-based therapies offer a wide range of therapeutic interventions including for the treatment of skin diseases; however, the strategies to deliver efficiently these biomolecules are still limited due to obstacles related to the cellular uptake and cytoplasmic delivery. Herein, we synthesized a triggerable polymeric nanoparticle (NP) library composed by 160 formulations, presenting physico-chemical diversity and differential responsiveness to light. Six formulations were more efficient (up to 500%) than commercial Lipofectamine in gene knockdown activity. These formulations had differential internalization by skin cells and the endosomal escape was rapid (minutes range) as shown by the recruitment of galectin-8. The NPs were effective in the release of siRNA and miRNA. Acute skin wounds treated with the top hit NP complexed with miRNA-150-5p healed faster than wounds treated with scramble miRNA. Light-activatable NPs offer a new strategy to deliver topically non-coding RNAs.

The capacity to regulate intracellular gene expression with RNA-based therapeutics such as small interfering RNAs (siRNAs) or miRNAs has enormous potential for the treatment of many diseases ^[1]. Unfortunately, the intracellular delivery of RNA-based therapeutics is difficult because of their susceptibility to enzymatic degradation and low capacity to cross cell membrane without a vector/carrier. Several delivery

strategies have been developed in the last years for the rapid (to facilitate *in vivo* translation) and efficient (to escape the endolysosomal compartment) delivery of RNA-based therapeutics based on NPs, scaffolds, nano-needles, among others ^[1]. NPs that either encapsulate or carry RNA-based therapeutics in their surfaces can stabilize the RNA molecules, target potentially specific cell populations and deliver intracellularly the cargo. Unfortunately, NP formulations still offer limited success in terms of endolysosomal escape and temporal delivery of the cargo ^[2]. For example, in the most efficient formulations, the escape of RNA molecules from the endolysosomal compartment is below 2% ^[1c, 3]. Moreover, with the exception of few cases ^[4], most of the formulations do not allow temporal delivery of the cargo and yet this issue seems very important, because for effective knockdown, RNA molecules should be released from the endosomal compartment shortly (≈ 15 min) ^[3] after endocytosis.

The hypothesis of this study is that rapid and efficient delivery systems for RNA intracellular delivery requires the development of NP libraries for the identification of formulations that facilitate cell internalization while enabling temporal control in the delivery of RNA, with potential advantages in terms of endolysosomal escape. Previous studies have used high-throughput screening to identify NPs to release intracellularly non-coding RNAs ^[5]; however, without enabling remote control by an external stimulus such as light. Several strategies have been reported to make light-triggerable NP delivery systems ^[6]. A frequently used approach is to introduce light cleavable molecules, such as *o*-nitrobenzyl groups, on the polymer backbone ^[7]. Light exposure of the NPs leads to the cleavage of the photo-sensitive moiety followed by the disassembly of the formulation.

Here, we have prepared and characterized a light-triggerable NP library for the controlled intracellular delivery of RNA-based therapeutics. The preparation of such NP library required the use of simple synthetic schemes to be implemented in a high-throughput way, avoiding long purification steps. Thus, we have selected Michael-type addition chemistry to produce polymers with chemical diversity ^[3, 5a, 5c]. We have synthesized a photo-cleavable linker, based on *o*-nitrobenzyl chemistry, which was reacted with a set of bisacrylamide and amine monomers. The synthesized polymers were precipitated in water to form NPs and then complexed with non-coding RNAs (siRNA or miRNAs). The NPs were characterized for their size, zeta potential, light disassembly properties, cellular internalization and gene knockdown activity. The formulations with high

activity were characterized for their endolysosomal escape. For proof of concept, we demonstrated the efficacy of the formulation in a skin wound healing animal model using miRNA-150-5p, a miRNA recently identified by us to be involved in keratinocyte proliferation and migration as well as skin fibroblast survival in ischemic conditions.^[8] To the best of our knowledge, there are only three studies reporting the use of light-triggerable formulations for the delivery of miRNAs *in vivo*. In one of the studies, the miRNA was modified with a photolabile caging group sensitive to UV-light^[9] and showed limited skin regeneration at macroscopic level. The other studies reported a formulation sensitive to NIR light for the delivery of miRNAs^[4e, 10]; however, the inorganic nature of the formulation raises some issues for a potential clinical translation. Here we have identified a biodegradable NP formulation that is able to transfect efficiently *in vivo* miRNAs and enhance significantly wound healing kinetics.

To confer the light sensitivity to the polymers, a photo-cleavable linker P1 was introduced in polymer backbone (Figs. S1A and S1B). The library was prepared by the addition of monomers (P1, amine and bisacrylamide monomers) in dimethyl sulfoxide (DMSO), for 5 days, at 60 °C (Figs. 1A-1C). To confer high light sensitivity to the synthesized polymers (and consequently NPs) the ratio of P1 per repeating unit of the polymer was 25 (P1):25 (bisacrylamide):50 (diamine) (Figs. S1C and S1D). At the end of the reaction, the unreacted acrylamide groups were capped with amines since previous studies have demonstrated that amine-terminated polymers had higher transfection efficiencies^[11]. The efficiency of the capping procedure was high as no measurable acrylate proton signals (5 – 7 ppm) were observed by ¹H-NMR (Fig. S1C and Fig. S2). The synthesized polymer library had (i) a large variety of side groups (ii) disulfide bonds that were relative stable in physiological conditions (pH 7.4) but were rapidly degraded in intracellular reductive environments and (iii) different solubility and hydrophilicity in aqueous solution.

The library of 160 polymers was then precipitated in water to form NPs (Fig. S3A). In the conditions tested, most of the polymers (90%) were able to form NPs. Polymers that failed NP formation were either soluble in water or formed large polymeric aggregates. The average yield of NP formation was $20.7 \pm 15.3\%$, having 10% of the polymers yields above 25% (Fig. S3B). 90% of the NPs had a size range between 100 and 500 nm (Fig. S3C) and 20% of the NPs a zeta potential above 20 mV (Figs. S3D-S3E), as evaluated by dynamic light scattering (DLS). TEM analyses confirmed the size range obtained by DLS (Fig. S4). The light

responsiveness of the NPs was then evaluated by the quantification of number of counts per second before and after light exposure, as assessed by DLS (Fig. S3F), and by TEM analyses (Fig. S4). Approximately 80% of the formulations showed 50% count decrease after 10 min of UV light exposure. Light sensitivity seemed to be independent on the characteristics of the bisacrylamide monomers.

To form the NP@siRNA complexes, both NP and siRNA were mixed to promote electrostatic interactions. Based on preliminary tests with P1C5 formulation, a ratio siRNA (against GFP): NP (w/w) of 1:50, a concentration of NP@siRNA of 20 $\mu\text{g}/\text{mL}$ and a transfection time of 10 min were selected for running the NP library (Fig. S5). For *in vivo* applications (see below), it is desirable that the formulations are rapidly internalized by cells to reduce their clearance from the place they are administered and thus a 10 min-transfection time was used for subsequent studies. To run the library, the NPs were complexed with siRNA labeled with a Cy5 tag, followed by the centrifugation of the NPs, the quantification of the concentration of siRNA not immobilized onto the NPs in the supernatant, and the use of NP@siRNA complexes for cell transfection (Fig. S6A). In average, $79.0 \pm 13.5\%$ of the initial siRNA was immobilized onto the NPs. Thirty two percent of the formulations did immobilize more than 80% of the initial siRNA (Fig. S6B). Formulations more effective binding siRNA were those NPs formed by bisacrylamide A, C and E and diamines 2, 3, 4, 5, 6, 7, 11, 16, 21 or 22. Our results suggested that the binding of siRNA was not only dependent on positive zeta potential but also on the presence of aliphatic moieties in the polymer backbone.

To evaluate the knockdown properties of the NP@siRNA complexes, HeLa cells stably expressing eGFP were transfected with the formulations. Cells were transfected with NP@siRNA-Cy5 (siRNA:NP 1:50; 20 $\mu\text{g}/\text{mL}$) complexes for 10 min, washed to remove non-internalized complexes, either irradiated or not for 10 min and cultured for additional 48 h. Lipofectamine was used as control. High-content imaging was used to monitor simultaneously several parameters in the same screening experiment, such as cell viability, NP internalization (from the Cy5 tag of the siRNA) and GFP knockdown (Fig. S7). For the concentration tested, the formulations had no significant impact in cell viability (cell viability > 90%) (Fig. S6C) but they showed significant differences in the delivery of siRNA within cells (Fig. S6D). It is interesting to note that although some formulations showed higher cell uptake (e.g. P1A19 formulation) than others (e.g. P1C7 formulation) they showed lower GFP knockdown. It is possible that differences in NP disassembly after light activation

(34% decrease in P1A19 vs. 88% in P1C7) as well as in NP zeta potential (25.9 ± 0.5 mV in P1A19 vs. 18.9 ± 0.9 mV in P1C7) may result in variable siRNA release after NP disassembly (Figs. S6E and S6F) and ultimately biological activity. Importantly, six formulations were more efficient than commercial Lipofectamine to knockdown GFP (Fig. 1D). These formulations contained bisacrylamide A (shortest aliphatic), C (bio-reducible disulphide bond) and diamines 1 (short aliphatic), 4-7 (increased nitrogen content) and 10-11 (ethyleneglycol containing units) (Table S1). Two formulations (P1C7 and P1C5) were selected for further characterization due to their high ability to knock down the reporter cell line. Importantly, the knock down activity of the formulations was superior after light activation as compared to the same formulations without light activation, highlighting the temporal control of their biological activity. P1C7 formulation was the most promising one because of its efficiency and temporal control of GFP knockdown (Table S2). The internalization of P1C7@siRNA-Cy5 NPs in HeLa cells was endocytic and mainly mediated by scavenger receptors (Fig. S8).

Light-triggerable NPs might have potential use in skin applications [4e, 10]. Therefore, we evaluated whether some of the formulations had different tropism to skin cells. For this purpose, the internalization of 2 formulations with high GFP knockdown (P1C7 and P1C5) as well as one formulation with low GFP knockdown (P1D30) were tested against human skin cells, specifically, fibroblasts, keratinocytes and endothelial cells (ECs). Cells were transfected with NPs@siRNA-Cy5 or lipofectamine@siRNA-Cy5 (Fig. S9). Our results show significant differences in NP internalization according to each cell type demonstrating that cell internalization was dependent on the chemistry of the formulation. P1C7 formulation had higher tropism to fibroblasts and keratinocytes than ECs. Based on the knockdown efficiency (highest GFP knockdown after light irradiation, Fig.1D) and skin cell internalization pattern (high NP internalization in keratinocytes and fibroblasts (Fig.S9) which benefits the bioactivity of the non-coding RNA tested below), P1C7 NPs were selected for subsequent studies.

Previous studies have demonstrated that the efficacy of the RNA silencing mechanism is directly correlated with endosomal escape [1c, 5a], which is mediated by the recruitment of galectin-8 to the RNA releasing endosomes [3]. To evaluate whether the efficacy of P1C7 formulation in RNA silencing is connected to the rapid endosomal escape, the kinetics of galectin-8 recruitment was measured on A7r5-Gal8YFP reporter

cells [12]. Cells were transfected with P1C7@siRNA-Cy5 NPs for 10 min, after which, they were exposed to UV light for 10 min and then incubated for 60 min. Lipofectamine complexed with the same amount of siRNA-Cy5 was used as control. The area of siRNA-Cy5 NPs decreased overtime indicating the disassembly of the NPs within cells. Cells transfected with P1C7@siRNA-Cy5 showed a higher number of foci with galectin 8 than the ones transfected with lipofectamine, and the foci number as well as the foci area increased overtime (Figs. 2A and B). To further confirm these results, we have transfected HeLa cells for 10 min (followed or not by UV light exposure) with P1C7@siRNA-Cy5, Lipo@siRNA-Cy5 or a formulation with high cell uptake but low capacity for GFP knockdown (P1A19@siRNA-Cy5). Confocal microscopy results showed lower co-localization of P1C7@siRNA-Cy5 with the endolysosomal compartment (stained with LysoTracker) than Lipo@siRNA-Cy5 or P1A19@siRNA-Cy5 (Fig. S10). Overall, our results indicate that P1C7 formulation delivered more efficiently the siRNA to the cell cytoplasm than lipofectamine or other NP formulations.

To extend the application of P1C7 NPs, the formulation was used for the delivery of miRNAs. NPs were complexed with miRNA-150-5p (from now on termed as miRNA150). Cells were transfected with P1C7 NPs, P1C7 NPs@miRNA150 or lipofectamine@miRNA150 (Fig. 2C). Cells were then wounded and cell migration was monitored. At 48 h post wounding, cells transfected with non-irradiated P1C7 NPs@miRNA150 showed increased migration as compared to NPs without miRNA150 (Fig 2D.1 and Fig. S11). Importantly, cells transfected with P1C7 NPs@miRNA150 and activated by light showed increased migration as compared to cells transfected with non-activated NPs or lipofectamine, both complexed with miRNA150. As expected, the increased migration of cells seems to be mediated by an increase in the intracellular levels of miRNA150 (Fig. 2D.2) and by the knock down of the *cMYB* gene (Fig. 2D.3), a direct target of the miRNA [13].

Next, we evaluated whether P1C7@miRNA150 NPs could function *in vivo*, in an acute wound healing animal model. Initially, we investigated whether the formulation could be activated *in vivo* by a blue laser after subcutaneous transplantation (Figs. S12A and S12B). We have used a blue laser rather than a UV light (used in the *in vitro* tests) to prevent potential tissue damage. The blue laser (408 nm at 80 mW/cm²) led to similar levels of gene knockdown in cells transfected with P1C7@siRNA complexes as the UV light (365 nm

at 1 mW/cm²) (Fig. S12C). Our results show high NP disassembly even if the attenuation of the laser was significant (only 4% of the laser was able to cross the skin barrier of 300-400 μm) (Figs. S12B and S12C). Then, we administered P1C7 NPs@miRNA150 subcutaneously in the borders of wounds and allowed the NPs to be internalized by the skin tissue for 30 min, followed by their activation by a blue laser for 5 min (Fig. 3A). P1C7 NPs@scramble miRNA or vehicle (PBS) were used as controls. Wounds treated with light-triggered P1C7@miRNA150 NPs healed faster as compared to wounds treated with PBS or P1C7 NPs@scramble miRNA, being statistical significant for some of the days (Fig. 3B, Figure S13). These results were also confirmed by histological analyses showing qualitative differences in the wound healing process and re-epithelization (Figs. 3C and 3D). Wounds treated with PBS were in stages of inflammation and tissue formation until tissue remodeling, whereas wounds treated with P1C7 NPs@miRNA150 were all in the tissue remodeling phase (Fig. 3D). To show that indeed the regenerative program was mediated by miRNA150, the expression of the *cMYB* gene, a direct target of miRNA150, was evaluated at day 3 by qRT-PCR (Fig. 3E). The percentage of *cMYB* gene transcripts were 60% lower in wounds treated with P1C7@miRNA150 NPs than with P1C7 NPs.

In conclusion, we have successfully synthesized a light-activatable NP library for efficient *in vivo* small non-coding RNA delivery. The library screening revealed six formulations which were more efficient in cell transfection and RNA silencing as the commercial agent Lipofectamine with additional temporal control over the release of the small non-coding RNA. P1C7, as leading formulation, was shown to be a rapid transfection agent with fast endosomal escape and high efficiency not only for siRNA mediated gene silencing but also for microRNAs. Moreover, we demonstrate high efficacy and significance of light-triggered microRNA delivery in a wound healing animal model. Taken together, light-triggerable NP formulations give an extra level of control in the delivery of non-coding RNAs which may enhance their bioactivity.

ACKNOWLEDGEMENTS

The authors would like to thank the financial support of ERA Chair project (ERA@UC, ref:669088) through EU Horizon 2020 program, the POCI-01-0145-FEDER-016390 (acronym: CANCEL STEM) and POCI-01-0145-FEDER-029414 (acronym: LightBRARY) projects through Compete 2020 and FCT programs. NMR data was collected at the UC-NMR facility which is supported in part by FEDER – European Regional Development Fund through the COMPETE Programme (Operational Programme for Competitiveness) and

by National Funds through FCT – Fundação para a Ciência e a Tecnologia (Portuguese Foundation for Science and Technology) through grants REEQ/481/QUI/2006, RECI/QEQ-QFI/0168/2012, CENTRO-07-CT62-FEDER-002012, and Rede Nacional de Ressonância Magnética Nuclear (RNRMN).

- [1] aR. L. Juliano, *Nucleic Acids Res* **2016**, *44*, 6518-6548; bS. F. Dowdy, *Nat Biotechnol* **2017**, *35*, 222-229; cJ. Gilleron, W. Querbes, A. Zeigerer, A. Borodovsky, G. Marsico, U. Schubert, K. Manygoats, S. Seifert, C. Andree, M. Stoter, H. Epstein-Barash, L. Zhang, V. Kotliansky, K. Fitzgerald, E. Fava, M. Bickle, Y. Kalaidzidis, A. Akinc, M. Maier, M. Zerial, *Nat Biotechnol* **2013**, *31*, 638-646.
- [2] R. Kanasty, J. R. Dorkin, A. Vegas, D. Anderson, *Nat Mater* **2013**, *12*, 967-977.
- [3] A. Wittrup, A. Ai, X. Liu, P. Hamar, R. Trifonova, K. Charisse, M. Manoharan, T. Kirchhausen, J. Lieberman, *Nat Biotechnol* **2015**, *33*, 870-876.
- [4] aR. Huschka, A. Barhoumi, Q. Liu, J. A. Roth, L. Ji, N. J. Halas, *ACS Nano* **2012**, *6*, 7681-7691; bY.-T. Chang, P.-Y. Liao, H.-S. Sheu, Y.-J. Tseng, F.-Y. Cheng, C.-S. Yeh, *Advanced Materials* **2012**, *24*, 3309-3314; cY. Yang, F. Liu, X. Liu, B. Xing, *Nanoscale* **2013**, *5*, 231-238; dG. B. Braun, A. Pallaoro, G. Wu, D. Missirlis, J. A. Zasadzinski, M. Tirrell, N. O. Reich, *ACS Nano* **2009**, *3*, 2007-2015; eH. Wang, P. Agarwal, S. Zhao, J. Yu, X. Lu, X. He, *Advanced Materials* **2016**, *28*, 347-355.
- [5] aG. Sahay, W. Querbes, C. Alabi, A. Eltoukhy, S. Sarkar, C. Zurenko, E. Karagiannis, K. Love, D. Chen, R. Zoncu, Y. Buganim, A. Schroeder, R. Langer, D. G. Anderson, *Nat Biotechnol* **2013**, *31*, 653-658; bK. A. Whitehead, J. R. Dorkin, A. J. Vegas, P. H. Chang, O. Veiseh, J. Matthews, O. S. Fenton, Y. Zhang, K. T. Olejnik, V. Yesilyurt, D. Chen, S. Barros, B. Klebanov, T. Novobrantseva, R. Langer, D. G. Anderson, *Nat Commun* **2014**, *5*, 4277; cK. L. Kozielski, S. Y. Tzeng, B. A. De Mendoza, J. J. Green, *ACS Nano* **2014**, *8*, 3232-3241; dJ. E. Dahlman, C. Barnes, O. Khan, A. Thiriout, S. Jhunjunwala, T. E. Shaw, Y. Xing, H. B. Sager, G. Sahay, L. Speciner, A. Bader, R. L. Bogorad, H. Yin, T. Racie, Y. Dong, S. Jiang, D. Sedorf, A. Dave, K. S. Sandu, M. J. Webber, T. Novobrantseva, V. M. Ruda, A. K. R. Lytton-Jean, C. G. Levins, B. Kalish, D. K. Mudge, M. Perez, L. Abezgauz, P. Dutta, L. Smith, K. Charisse, M. W. Kieran, K. Fitzgerald, M. Nahrendorf, D. Danino, R. M. Tudor, U. H. von Andrian, A. Akinc, A. Schroeder, D. Panigrahy, V. Kotlianski, R. Langer, D. G. Anderson, *Nat Nanotechnol* **2014**, *9*, 648-655; eC. Gehin, J. Montenegro, E. K. Bang, A. Cajaraville, S. Takayama, H. Hirose, S. Futaki, S. Matile, H. Riezman, *J Am Chem Soc* **2013**, *135*, 9295-9298.
- [6] Y. Zhou, H. Ye, Y. Chen, R. Zhu, L. Yin, *Biomacromolecules* **2018**.
- [7] P. Klan, T. Solomek, C. G. Bochet, A. Blanc, R. Givens, M. Rubina, V. Popik, A. Kostikov, J. Wirz, *Chem Rev* **2013**, *113*, 119-191.
- [8] H. Henriques-Antunes, R. M. S. Cardoso, A. Zonari, J. Correia, E. C. Leal, A. Jimenez-Balsa, M. M. Lino, A. Barradas, I. Kostic, C. Gomes, J. M. Karp, E. Carvalho, L. Ferreira, *ACS Nano* **2019**.
- [9] T. Lucas, F. Schafer, P. Muller, S. A. Eming, A. Heckel, S. Dimmeler, *Nat Commun* **2017**, *8*, 15162.
- [10] M. M. Lino, S. Simoes, A. Vilaca, H. Antunes, A. Zonari, L. Ferreira, *ACS Nano* **2018**.
- [11] A. Akinc, D. G. Anderson, D. M. Lynn, R. Langer, *Bioconjug Chem* **2003**, *14*, 979-988.
- [12] K. V. Kilchrist, B. C. Evans, C. M. Brophy, C. L. Duvall, *Cell Mol Bioeng* **2016**, *9*, 368-381.
- [13] C. Xiao, D. P. Calado, G. Galler, T. H. Thai, H. C. Patterson, J. Wang, N. Rajewsky, T. P. Bender, K. Rajewsky, *Cell* **2007**, *131*, 146-159.

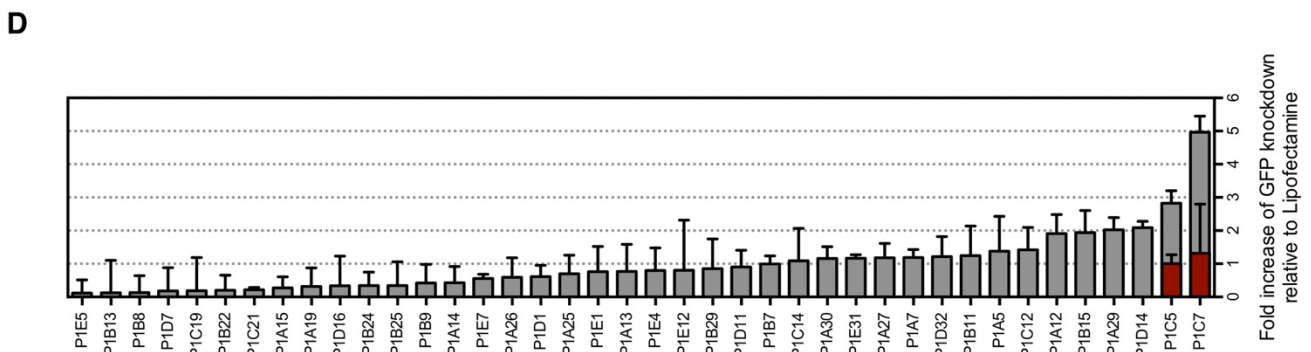
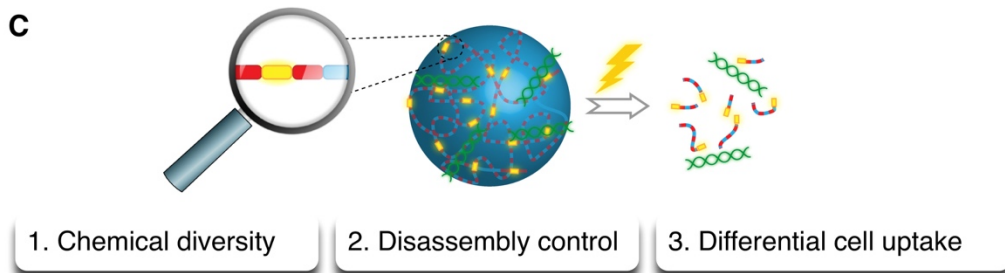
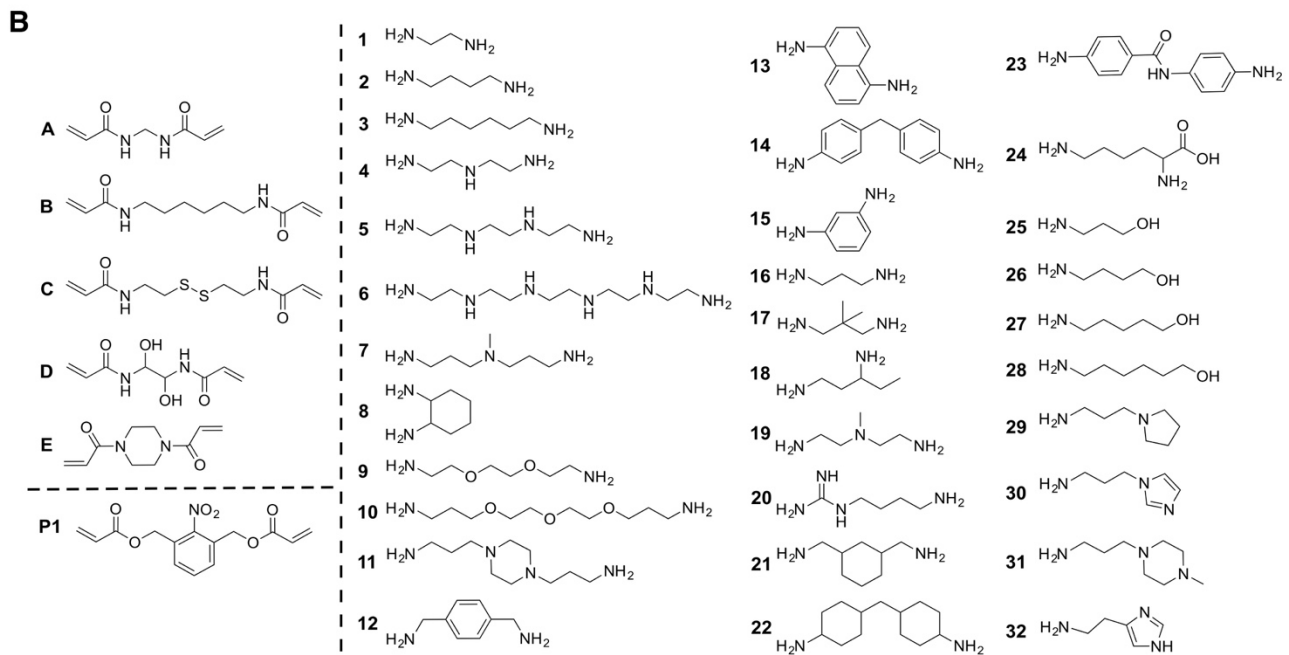
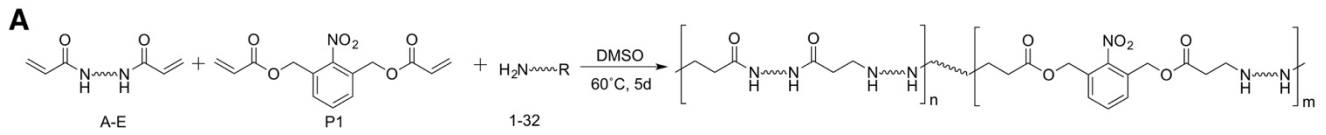


Figure 1. Light-triggerable NP library and gene knockdown activity. (A) Reaction scheme for the preparation of light-sensitive polymers based on the reaction of bisacrylamides (A-E), photo-cleavable diacrylate (P1) and amines (1-32). (B) Monomers used for the synthesis of the library. (C) Schematic representation of the light disassembly of the NPs. (D) High throughput screening of NPs for gene knockdown using siRNA. Fold increase of GFP knockdown after 48 h post transfection relative to Lipofectamine (Lipo) for the best 40 formulations. Cells were transfected with the formulations for 10 min and subsequently irradiated for 10 min with a UV lamp. The red bars show GFP knockdown in the best two formulations without UV irradiation. Results are expressed as Mean \pm SEM (n=3).

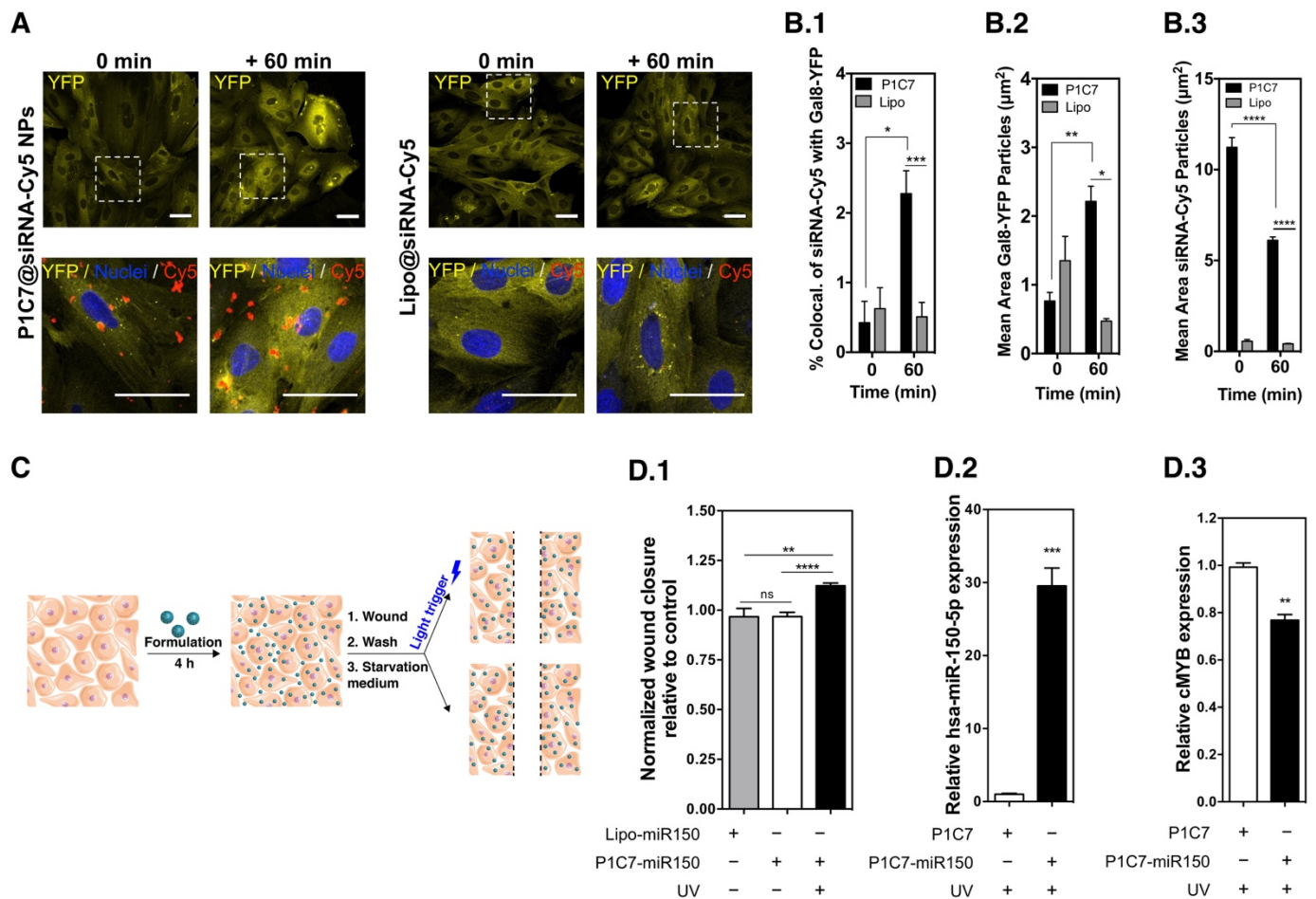


Figure 2. Intracellular trafficking and bioactivity. (A) Galectin-8 recruitment in A7r5-Gal8YFP reporter cells cultured in the presence of P1C7@siRNA-Cy5 or lipofectamine@siRNA-Cy5, as evaluated by confocal microscopy. Cells were transfected with the formulations for 10 min ($t = -10$ min) and then activated by UV light (10 min, 365 nm, 1 mW/cm²; $t = 0$ min). White scale bar is 50 μ m. (B) Colocalization of Galectin-8 YFP spots with Cy5 (B.1) as well as mean areas of bright Gal8-YFP spots (B.2) and siRNA-Cy5 (B.3). Results are Mean \pm SEM ($n=4-17$, 2 technical replicates). (C) Schematic representation of the experimental protocol. Confluent human keratinocytes were treated for 4 h with P1C7 NPs or P1C7@miR150 NPs. Lipofectamine complexed with miR150 was used as control. The wound was created by scratching the monolayer of cells. Cell migration was monitored by high-content microscopy. (D.1) Wound closure 48 h post-scratch. Wound area was quantified by ImageJ and normalized to the initial wound area. Results are presented as average \pm SEM ($n=6-8$). Quantification of miR150 (D.2) and *cMYB* (D.3) gene transcripts by qRT-PCR in keratinocytes treated with P1C7 NPs or P1C7@miR150 NPs, 48 h post wounding. Results are presented as Mean \pm SEM ($n=6-8$). Statistical analysis was performed by a student *t*-test, except for NP P1C7 against time at 0 min which was assessed by one-way ANOVA followed by a Bonferroni post-test. * $P < 0.05$; ** $P < 0.01$; *** $P < 0.001$; **** $P < 0.0001$.

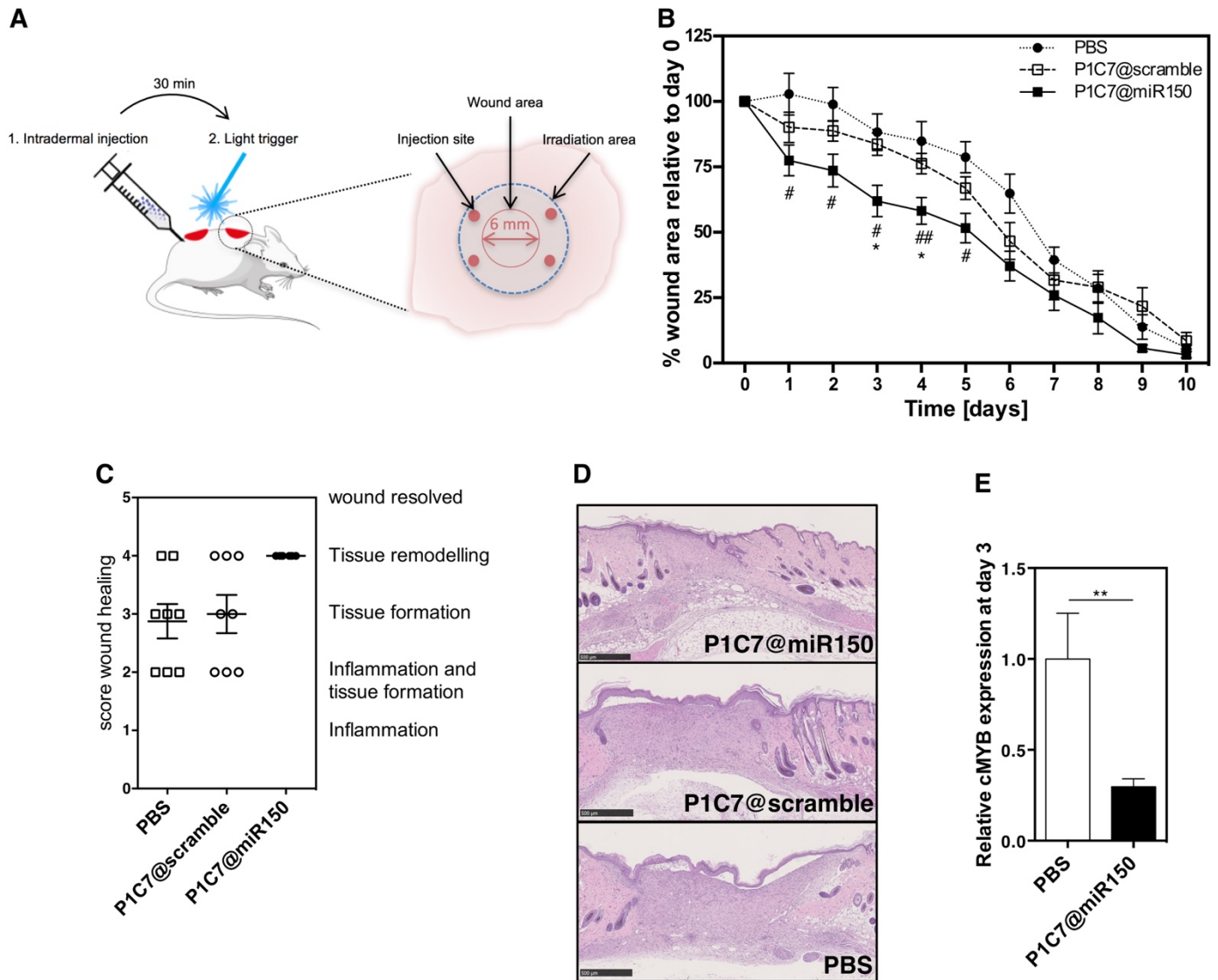
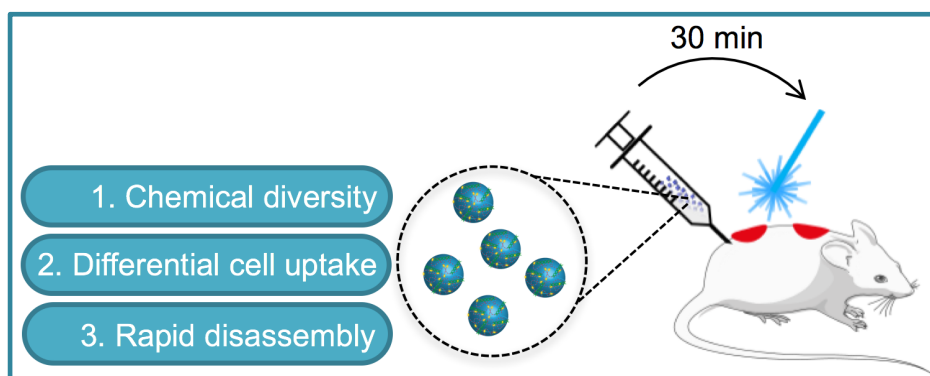


Figure 3. Acute wound healing activity of P1C7@miR150 formulation. (A) Schematic representation of the animal experimental set up. (B) Wound closure (relative to day 0) in animals treated with PBS, P1C7@scramble or P1C7@miR150. Results are Mean \pm SEM (n=8). Statistical analyses were performed by student t-test with Welch's correction. #P<0.05, ##P<0.01 between PBS and P1C7-miR150 groups; *P<0.05 between P1C7-scramble and P1C7-miR150 groups. (C) Histological score regarding wound healing. Results are Mean \pm SEM (n=8). (D) Representative hematoxylin/eosin staining's for wounds at day 10. Scale bar is 500 μ m. (E) Expression of *cMYB* transcripts in skin tissue quantified by qRT-PCR analyses. Data presented as Mean \pm SEM (n=6-20). ** P<0.01.

TABLE OF CONTENTS



A light-sensitive nanoparticle library was synthesized to deliver non-coding RNAs. Six formulations were more efficient (up to 500%) than commercial lipofectamine in gene knockdown activity. These formulations had differential internalization by skin cells and the endosomal escape was rapid (minutes range). We demonstrated the utility of these light-triggerable nanoparticles in the context of wound healing.